Journal of Visualized Experiments

Autoradiography as a simple and powerful method for visualization and characterization of pharmacological targets

--Manuscript Draft--

Article Type:	Invited Methods Article - JoVE Produced Video
Manuscript Number:	JoVE58879R2
Full Title:	Autoradiography as a simple and powerful method for visualization and characterization of pharmacological targets
Keywords:	radioligand, radioactive; autoradiography; affinity; expression; phosphor imaging; HOCPCA; γ-hydroxybutyric acid; GHB; NCS-382; quantitative pharmacology
Corresponding Author:	Petrine Wellendorph Kobenhavns Universitet Copenhagen, Denmark DENMARK
Corresponding Author's Institution:	Kobenhavns Universitet
Corresponding Author E-Mail:	pw@sund.ku.dk
Order of Authors:	Nane Griem-Krey
	Anders Bue Klein
	Matthias Herth
	Petrine Wellendorph
Additional Information:	
Question	**Response**
Please indicate whether this article will be Standard Access or Open Access.	Standard Access (US$2,400)
Please indicate the **city, state/province, and country** where this article will be **filmed**. Please do not use abbreviations.	Copenhagen, Denmark

Copenhagen Oct 21, 2018

Dear Editor

We have revised the manuscript according to the additional requests. The suggestions and questions have been addressed and incorporated into a revised manuscript and/or given as point-by-point comments in the rebuttal letter. Specific changes to the manuscript are indicated with 'red text'.

We look forward to the next step in the production of the video.

Sincerely, Petrine Wellendorph

Petrine Wellendorph
Associate Professor

Faculty of Health and Medical Sciences
Experimental Pharmacology
UNIVERSITY OF COPENHAGEN
Universitetsparken 2
2100 Copenhagen Ø
Denmark

TEL +45 3533 6397
pw@sund.ku.dk
www.drug.ku.dk

1 **TITLE:**
2 Autoradiography as a Simple and Powerful Method for Visualization and Characterization of
3 Pharmacological Targets
4
5 **AUTHORS & AFFILIATIONS:**
6 Nane Griem-Krey[1], Anders B. Klein[1], Matthias M. Herth[1,2,3], Petrine Wellendorph[1]
7 [1]Department of Drug Design and Pharmacology, Faculty of Health and Medical Sciences,
8 University of Copenhagen, Copenhagen, Denmark
9 [2]Neurobiology Research Unit and CIMBI, Copenhagen University Hospital, Copenhagen, Denmark
10 [3]Department of Clinical Physiology, Nuclear Medicine & PET, Copenhagen, Denmark
11
12 **Corresponding Author:**
13 Petrine Wellendorph
14 Email Address: pw@sund.ku.dk
15 Tel: +45 3533 6397
16
17 **KEYWORDS:**
18 Radioligand, radioactive, autoradiography, affinity, expression, phosphor imaging, HOCPCA, γ-
19 hydroxybutyric acid, GHB, NCS-382, quantitative pharmacology
20
21 **SHORT ABSTRACT:**
22 The method of autoradiography is routinely used to study binding of radioligands to tissue
23 sections for determination of qualitative or quantitative pharmacology.
24
25 **LONG ABSTRACT:**
26 *In vitro* autoradiography aims to visualize the anatomical distribution of a protein of interest in
27 tissue from experimental animals as well as humans. The method is based on the specific binding
28 of a radioligand to its biological target. Therefore, frozen tissue sections are incubated with
29 radioligand solution, and the binding to the target is subsequently localized by the detection of
30 radioactive decay, for example, by using photosensitive film or phosphor imaging plates.
31 Resulting digital autoradiograms display remarkable spatial resolution, which enables
32 quantification and localization of radioligand binding in distinct anatomical structures. Moreover,
33 quantification allows for the pharmacological characterization of ligand affinity by means of
34 dissociation constants (K_d), inhibition constants (K_i) as well as the density of binding sites (B_{max})
35 in selected tissues. Thus, the method provides information about both target localization and
36 ligand selectivity. Here, the technique is exemplified with autoradiographic characterization of
37 the high-affinity γ-hydroxybutyric acid (GHB) binding sites in mammalian brain tissue, with special
38 emphasis on methodological considerations regarding the binding assay parameters, the choice
39 of the radioligand and the detection method.
40
41 **INTRODUCTION:**
42 Autoradiography is a method which provides images of radioactive decay. The technique is
43 routinely used to study the tissue distribution of a protein of interest *in vitro* based on a specific
44 pharmacological interaction between a radiolabelled compound and its target. This provides

45 direct information about the selectivity of the ligand for the target. *In vitro* autoradiography may
46 also be used for quantitative determination of pharmacological binding parameters of
47 radioligands, such as the dissociation constant (K_d) and density of binding sites (B_{max}), as well as
48 for determining the inhibition constant (K_i) of competing ligands[1,2]. Compared to traditional
49 homogenate radioligand binding, autoradiography has the advantage of being able to visualize
50 spatial anatomy and giving succinct details of regional expression patterns[3]. The method of
51 autoradiography is therefore a relevant alternative to immunocytochemistry, especially in the
52 absence of a validated antibody. Autoradiography is easily implemented in a standard
53 radioisotope laboratory given the availability of a suitable radioligand with the required
54 pharmacological specificity, access to a microtome cryostat for preparing tissue sections, and a
55 suitable imaging device that is able to analyze the distribution of radioactivity in the respective
56 tissue sections. Notably, an important selection criterion for the radioligand is a limited amount
57 of binding to non-target sites. This can be to other proteins, membranes or materials such as
58 plastic or filters, and is collectively referred to as non-specific binding. Usually, non-specific
59 binding is non-saturable but can be saturable if it involves a specific off-target protein. The best
60 way of validating true specific binding is to compare to tissues lacking the target, *e.g.*, genetically
61 engineered (knock-out) tissue[4].
62
63 Here, the methodology is illustrated with the autoradiographic characterization of the high-
64 affinity binding site for γ-hydroxybutyric acid (GHB) in the mammalian brain. Understanding the
65 pharmacological interaction between GHB and its binding site is of relevance as GHB is both a
66 clinically useful drug in the treatment of narcolepsy and alcoholism[5], but also a natural
67 constituent of the mammalian brain and a recreational drug[6]. High-affinity GHB binding sites
68 were first described using [3H]GHB binding to rat brain homogenate[7]. Over the years, further
69 autoradiography studies with [3H]GHB and the analogue [3H]NCS-382 has showed a high density
70 of binding sites in forebrain regions of rat[8–10], mouse[9], pig[11] and monkey/human brain[12].
71 However, the molecular identity and exact functional relevance of these binding sites have
72 remained elusive.
73
74 With the intention to further characterize the binding sites, and to facilitate studies on the
75 physiological role of GHB, multiple radioligands incorporating different isotopes endowed with
76 different affinities have been developed ([3H]GHB, [3H]NCS-382, [3H]HOCPCA and [125I]BnOPh-
77 GHB)[13–16] (reviewed in[17]) (**Figure 1**). The combination of selective high-affinity radioligands and a
78 very high tissue density of the binding sites have allowed for the production of high-quality
79 images using the phosphor imaging technique[9,11]. Along with an outline of the practical points in
80 setting up an autoradiographic experiment and an illustration to exemplify details, the discussion
81 section will emphasize i) the choice of radionuclide, ii) the choice of assay conditions, and iii) the
82 use of phosphor imaging plates versus X-ray film. The overall goal of this paper is to provide
83 technical, methodological and scientific details on the autoradiography technique for informing
84 about tissue distribution and pharmacological analysis of protein targets.
85
86 **PROTOCOL:**
87 All animal handling was performed in compliance with the guidelines from The Danish Animal
88 Experimentation Inspectorate.

89

90   NOTE: The protocol described here covers tissue preparation (*i.e.*, mouse brain tissue), the *in*
91   *vitro* autoradiographic assay in sufficient detail for setting up the method in a new lab, the
92   exposure to phosphor imaging plates as well as subsequent densitometric analysis of
93   autoradiograms (**Figure 2**) with the aim of localizing and quantifying radioligand binding in
94   distinct anatomical structures. For histological comparison, a protocol for cresyl violet staining is
95   included. Moreover, the determination of non-specific binding with a competing ligand is
96   included within the protocol. For a detailed description on how to determine K_d, B_{max} or K_i, see
97   previous publication[4].

98

99   **1.   Tissue Preparation by Cryosectioning**

100

101   1.1.   Euthanize the mouse by cervical dislocation and immediately dissect out the brain using
102   scissors and forceps. Directly proceed to the next step to avoid tissue damage.

103

104   1.2.   Snap-freeze the tissue by submersion in powdered dry ice, gaseous CO_2 or isopentane.
105   Directly transfer the frozen tissue to a cryostat with the temperature set to -20 °C. Alternatively,
106   store the tissue at -80 °C until processing.

107

108   NOTE: Avoid repeated thawing/freezing to reduce tissue damage.

109

110   1.3.   Let the tissue acclimate to -20 °C in the cryostat for 20 min before further processing to
111   avoid tissue shattering.

112

113   1.4.   Cover the tissue holder with embedding medium outside the cryostat and quickly place
114   the frozen tissue specimen in the desired orientation while the embedding medium is still liquid.
115   For instance, place the mouse brain vertically onto cerebellum in order to achieve rostral coronal
116   sections. Transfer the tissue holder back to the cryostat and expose the embedding medium to
117   temperatures below -10 °C for hardening.

118

119   NOTE: Fragile tissue specimen should be coated in embedding medium within the tissue molds
120   prior to mounting.

121

122   1.5.   Position the tissue holder in the microtome of the cryostat. Adjust the orientation of the
123   tissue to avoid sloped sections.

124

125   1.6.   Cut the tissue with the guidance of a stereotaxic atlas[18] in sections of desired thickness
126   (12 µm recommended for [³H] labelled ligands). Carefully straighten and unfold the section with
127   a brush of small size if necessary and thaw-mount the section onto a microscope slide.
128   Sequentially collect the sections from the region of interest for desired technical replication (*e.g.*,
129   4 sections per slide).

130

131   1.7.   Allow the sections on the slides to air-dry for 1 h before further handling.

132

NOTE: Addition of desiccant material to slide boxes minimizes moisture build up on the tissue sections. Procotol can be paused here by storing sections long-term in slide boxes at -80 °C.

2.   *In vitro* Autoradiography

CAUTION: Radioactivity. Work in a certified laboratory according to local regulations. Wear protective clothing. Dispose in accordance with radioactive decay or outsource to a certified company.

2.1.   Thaw the sections for at least 30 min at room temperature (RT). Label the slides with experimental conditions. Use a pencil because the slides will be bathed in ethanol during subsequent staining.

2.2.   Place the slides horizontally in plastic trays.

NOTE: Positioning slides on an elevated platform within plastic trays facilitates their handling.

2.3.   Pre-incubate the sections mounted on the slides in assay buffer adjusted to target in question (for GHB protocol, 50 mM $KHPO_4$ buffer pH 6.0 is used) by carefully applying an appropriate volume onto the slide (700 µL for 3-4 rodent coronal sections).

NOTE: Make sure that every section is covered completely with liquid.

2.3.1. Cover the plastic trays with a lid in order to avoid evaporation and pre-incubate at relevant temperature (for GHB protocol pre-incubate for 30 min at RT) under constant gentle (20 rpm) shaking on a plate shaker.

2.3.2. For the determination of non-specific binding, supplement assay buffer with relevant concentration of unlabelled compound (for GHB protocol, 1 mM GHB).

NOTE: Pre-incubation may not be necessary.

2.4.   Pour off pre-incubation liquid from each slide and transfer the slides back to the plastic tray.

2.5.   To avoid dehydration, immediately incubate the sections with relevant concentration of radioligand in assay buffer under desired conditions (for GHB protocol, 1 nM [^{3}H]HOCPCA for 1 h at RT) by covering the sections completely with the radioligand solution (700 µL for 3-4 rodent coronal sections).

2.5.1. Incubate under under constant gentle (20 rpm) shaking of plastic trays with closed lid.

NOTE: The radioligand concentration can be validated by counting an aliquot in a liquid scintillation counter.

2.6.   Remove the incubation solution by pouring off the liquid and transfer the slides into a microscope slide rack. Immediately proceed to the next step to avoid section dehydration.

2.7.   Wash the slides. For the GHB protocol, wash with ice-cold assay buffer twice for 20 s and then rinse twice by dipping the slide rack into the trays filled with ice-cold distilled water to remove salts. Position the slides vertically in racks for air-drying for at least 1 h at RT or dry the slides for 5 min with a blower set to cold temperature.

NOTE: Washing must be optimized, *e.g.*, extensive washing may be useful for decreasing non-specific binding.

2.8.   Transfer the slides to a fixator containing paraformaldehyde (PFA) powder for overnight fixation with PFA vapours at RT in order to protect the integrity of the ligand-target complex.

CAUTION: PFA is toxic. Positionthe fixator in fume hood and avoid skin/eye contact with PFA.

2.9.   The following day, transfer the slides to a desiccator box containing silica gel for 3 h at RT to eliminate moisture.

3.   Exposure to Phosphor Imaging Plates and Scanning

3.1.   Place the sections in a radiation-shielded imaging plate cassette with the tissue facing up. For subsequent quantification of radioligand binding, include a [^{3}H]microscale in every cassette. Arrange the sections randomly and expose the sections for direct comparison in the same cassette.

3.2.   Erase the tritium-sensitive phosphor imaging plate immediately before usage in order to remove accumulated signals from storage and to eliminate background signals. Therefore, load the plate into phosphor imaging machine and expose it to visible/infrared light according to the instructions of the manufacturer.

3.3.   Remove the plate from phosphor imaging machine and immediately place it onto the sections in the cassette. Make sure that the cassette is closed completely. Expose the sections to the phosphor imaging plate for 3 days at RT shielded from light.

3.4.   Because light erases signal from the imaging plate, carefully open the cassette in the dark and immediately transfer the imaging plate into the dark box of a phosphor imager or place the phosphor imager in a dark room.

NOTE: Make sure to notate the spatial arrangement of the slides during exposure in order to identify individual specimen on the digital image after analysis. Therefore, phosphor imaging plates also display one corner cut in a distinct angle in order to identify the correct orientation of the plate on the digital picture.

221

223

4.   Optional: Cresyl Violet Staining of Tissue Sections

225

4.1.   Prepare 1% cresyl violet solution by mixing 5 g of cresyl violet acetate in 500 mL of deionized water (dH$_2$O) until dissolved (approximately 2 h). Filter through a filter paper using a funnel into a new 500 mL bottle. Adjust pH to 3.5-3.8.

229

4.2.   Position the slide staining set under fume hood. Prepare trays with the following solutions in white polypropylene trays (except for xylene):

a.   50% ethanol/50% dH$_2$O
b.   70% ethanol/30% dH$_2$O
c.   100% ethanol
d.   100% ethanol
e.   100% dH$_2$O
f.   1% cresyl violet
g.   0.07% acetic acid (add 175 μL of acetic acid to 250 mL of dH$_2$O).
h.   100% xylene in green solvent-resistant trays
i.   100% xylene in green solvent-resistant trays

241

4.3.   Transfer the slides to the fume hood and place them in a slide rack.

243

4.4.   Dissolve the lipids through increasing graded series of ethanol in dH$_2$O into 100% ethanol (tray a-d) by dipping the slides for 1 min.

246

4.5.   Rehydrate the specimens to dH$_2$O through descending concentrations of ethanol (tray a-d in reverse order, followed by tray e) by dipping the slides for 1 min.

249

4.6.   Immerse the specimens in cresyl violet solution for 10 min.

251

4.7.   Rinse the specimens in 0.07% acetic acid by lifting the slides up and down gently for 4-8 s. Wash the slides by dipping in dH$_2$O for 1 min.

254

4.8.   Dehydrate the specimens by immersion of the slides for 30 s in ascending concentrations of ethanol (tray a-d).

257

4.9.   Transfer the specimens through two trays of 100% xylene (tray h and i) to quench the ethanol.

260

4.10.   Rehydrate the specimens to dH$_2$O through descending concentrations of ethanol (tray a-d in reverse order, followed by tray e) by dipping the slides for 1 min.

263

264   4.11.   Remove the slides from saline with forceps. Add a few drops of organic solvent mounting
265   media per slide and add a 24 x 60 mm coverslip on top to protect specimens. Remove air bubbles
266   between the specimen and coverslip by gently pressing onto the coverslip.
267
268   NOTE: Keep the remaining slides in xylene during mounting to prevent drying.
269
270   4.12.   Dry the slides overnight in a fume hood at RT.
271
272   4.13.   Obtain a picture of specimen with a microscope and 1.25X objective.
273
274   **5.   Densitometric Analysis of Digital Image**
275
276   5.1.   Measure relative optical densities (RODs) of each calibration standard from the
277   [^{3}H]microscale with an image analysis software.
278
279   5.1.1.   Select an area of equal size for each point of the [^{3}H]microscale using a tool for **Region**
280   **creation** from the menu item **Region determination**. Assign a number to each selected area by
281   clicking on **Number** under the menu item **Label**.
282
283   5.1.2.   Export OD values for each point of the calibration standard by clicking **File | Export | 2D**
284   **region report**. Transfer ROD values to a spreadsheet and normalize by the size of the selected
285   area. Perform linear regression to obtain a standard curve for further densitometric analysis.
286
287   NOTE: Make sure that the selected areas are labelled in order to identify matching ROD values
288   and samples.
289
290   5.2.   Perform quantification of autoradiograms using the proprietary imaging software by
291   selecting the region of interest (ROI) using a **Region creation** tool in every section and measuring
292   its ODs. Select the same region in every section by creating a template for the region of interest,
293   which is copied and manually adjusted to minor variations in brain anatomy for each
294   autoradiogram. Identify the anatomy of the ROI by comparison of autoradiograms with a brain
295   atlas[18]. When multiple treatments are compared, perform the analysis blinded and randomized
296   in order to avoid biased selection of ROIs.
297
298   5.3.   Export ROD values and sizes of selected areas into a spreadsheet by clicking **File | Export**
299   **| 2D region report**.
300
301   5.4.   Divide the measured ROD of the selected ROI by its area to obtain the density per specific
302   area.
303
304   5.5.   Measure the ROD of the background of the plate and export corresponding ROD values
305   and area size into a spreadsheet. Subtract the average background signal from every ROD value
306   of each ROI.
307

308　5.6.　Average the RODs of technical replicates, *i.e.*, section replicates using tissue from the
309　same animal.

310

311　5.7.　Use the standard curve to convert RODs into units of radioligand binding, *i.e.*, nCi/mg
312　tissue equivalents (TE).

313

314　NOTE: The term TE is used because standards are generated with materials simulating tissue.

315

316　5.8.　Express binding by conversion of nCi/mg to fmol/mg TE according to the specific activity
317　of the radioligand (Equation 1).

$$
318 \qquad \text{ligand binding}\left[\frac{\text{fmol}}{\text{mg}}\ \text{TE}\right] = 1000 * \frac{\text{binding}\left[\frac{\text{nCi}}{\text{mg}}\ \text{TE}\right]}{\text{specific activity}\left[\frac{\text{Ci}}{\text{mmol}}\right]} \qquad\qquad (1)
$$

319

320　5.9.　To obtain specific binding values, subtract non-specific binding from total binding.

321

322　5.10.　Average the binding of every biological replicate by using the average of the technical
323　replicates of each animal (obtained in Step 5.6).

324

325　**REPRESENTATIVE RESULTS:**
326　Using the described protocol, the anatomical distribution of the high-affinity GHB binding sites
327　was visualized with the radiolabelled GHB analogue [3H]HOCPCA in mouse brain, which was cut
328　into coronal, sagittal and horizontal sections (**Figure 3**). High levels of binding were observed in
329　hippocampus and cortex, lower binding in striatum and no binding was detected in cerebellum,
330　corresponding to previous reported expression patterns of the high-affinity GHB sites[9–12]. As
331　shown here, the anatomical structures may be visualized using different sectioning planes and
332　anatomical integrity may be supported by cresyl violet staining. For GHB high-affinity binding
333　sites, especially regions with low radioligand binding, such as cerebellum, are confirmed with
334　subsequent staining of the tissue (**Figure 3**). Coronal sections are most often found in the
335　literature[9,10]. They are practical for quantitative purposes as a higher amount of sections can be
336　obtained from one brain. Sagittal and horizontal sections have the advantage of visualizing
337　binding throughout most of the rodent brain within one section thus providing great overview.
338　**Figure 4** illustrates the evolutionary conservation of the high-affinity GHB binding sites in the
339　mammalian brain. [3H]HOCPCA binding sites were detected in mouse, rat as well as in pig brain
340　tissue enabling comparison of gross brain anatomy between species. Generally, evolutionary
341　conservation and regional distribution studies may aid significantly in the characterization of a
342　protein of interest, in this case a novel target, and may thus give indications about its
343　physiological function[19].

344

345　The high-affinity GHB binding sites were probed with GHB radioligands, which display different
346　affinities for the binding sites but comparable specific activities (**Figure 5**). [3H]HOCPCA was
347　previously shown to have a K_d of 74 nM, which is superior to the commercially available
348　radioligand [3H]NCS-382 with a K_d of 697 nM, both determined at pH 6.0 by quantitative
349　autoradiography[9]. Thus, [3H]HOCPCA is endowed with much higher sensitivity, leading to an

350 excellent signal-to-noise ratio. Due to the lower sensitivity of [³H]NCS-382, higher radioligand
351 concentrations must be used in order to obtain similar levels of binding (compare y-axes in **Figure**
352 **5**). When compared to [³H]GHB, even higher radioligand concentrations (30 nM) are necessary
353 to achieve comparable binding levels. This is predominantly due to the significantly lower affinity
354 (K_i of 4.5 µM) of this radioligand[20]. However, higher radioligand concentration also increases the
355 level of non-specific binding[9,10] with a consequently lower signal-to-noise ratio. This series of
356 experiments highlights the importance of having a high-affinity radioligand for producing high-
357 quality images.
358
359 Because the high-affinity GHB sites are expressed to so high levels in forebrain regions (60
360 pmol/mg[17]), the determination of pharmacological parameters by saturation curves is inherently
361 difficult using standard tritium sensitive phosphor imaging plates due to the risk of oversaturated
362 images. Therefore, K_d values for [³H]HOCPCA and [³H]NCS-382 have been obtained by first
363 determining K_i values by homologous displacement curves, and then calculation of K_d (**Figure 6**)[9].
364 For most radioligands, an alternative would be to use isotope-dilution as is routinely done in
365 homogenate binding assays. Moreover, K_d values have been determined at different pH values.
366 Evidently, the high-affinity GHB sites are most efficiently labelled at pH 6.0 (**Figure 6A** and **Figure**
367 **6D**), since changing assay conditions to pH 7.4 substantially impact ligand affinity. Thus, the K_d
368 for [³H]HOCPCA at pH 7.4 is approx. 30 times higher numerically than that at pH 6.0. Increasing
369 the pH further results in a higher degree of non-specific binding, which becomes a caveat when
370 using [³H]NCS-382 where only low amounts of specific binding can be obtained at pH 7.4 (**Figure**
371 **6E**). This in fact hinders the determination of pharmacological parameters using this radioligand
372 at physiological pH[9], again illustrating the power in having a radioligand with as high affinity as
373 possible.
374
375 **FIGURE LEGENDS:**
376 **Figure 1: Structures of radioligands targeting the high-affinity GHB binding sites.** [³H]3-
377 hydroxycyclopent-1-ene carboxylic acid ([³H]HOCPCA)[14], [³H](*E,RS*)-6,7,8,9-tetrahydro-5-
378 hydroxy-5*H*-benzocyclohept-6-ylidene acetic acid (NCS-382) ([³H]NCS-382)[15] and [³H]γ-
379 hydroxybutyric acid ([³H]GHB)[16] as tritiated radioligands with comparable specific activity (20-40
380 Ci/mmol), as well as [¹²⁵I]4-hydroxy-4-[4-(2-iodoben-zyloxy)phenyl]butanoate ([¹²⁵I]BnOPh-
381 GHB)[13] with an estimated molar activity of 2000 Ci/mmol[21]. The GHB structural element is
382 highlighted in red.
383
384 **Figure 2: Schematic overview of the protocol of *in vitro* autoradiography.** (1) The animal is
385 euthanized, tissue is dissected and snap-frozen on dry ice. Tissue is then sectioned on a cryostat,
386 thaw-mounted onto microscope slides and (2) sections are incubated with radioligand until
387 equilibrium binding. For determination of non-specific binding, solutions are supplemented with
388 an unlabelled displacer of a related but not identical chemical structure. (3) Subsequently,
389 unbound radioligand is removed by washing in assay buffer and salts are eliminated by rinsing
390 with distilled H_2O. When sections are dry, paraformaldehyde (PFA) fixation is performed to
391 permanently establish the ligand-protein interaction. Sections are then exposed to phosphor
392 imaging plates. (4) After sufficient exposure time, plates are scanned to obtain digital
393 autoradiograms. (5) Ultimately, image analysis is performed using definitions of regions of

394 interest (ROIs), and the binding is quantified. In the shown example, optical densities (ODs) are
395 illustrated in sections of mouse cortex (left) and hippocampus (middle). Quantification is done by
396 exposing sections together with a [^{3}H]microscale (right).
397
398 **Figure 3: Representative autoradiograms of 1 nM [^{3}H]HOCPCA binding to mouse brain sections.**
399 (**A**) Radioligand binding to coronal, sagittal and horizontal tissue sections to illustrate the
400 importance of the sectioning plane on the visibility of anatomical structures. (**B**) Cresyl violet
401 staining of corresponding tissue sections to verify anatomical regions, particularly regions with
402 low/absent radioligand binding.
403
404 **Figure 4: Representative autoradiograms of 1 nM [^{3}H]HOCPCA binding in different species.**
405 Comparison of (**A**) rat, (**B**) mouse and (**C**) pig *in vitro* autoradiograms in order to illustrate
406 evolutionary conservation of binding sites to cortical and hippocampal regions along with gross
407 brain anatomy.
408
409 **Figure 5: Quantification of binding to the high-affinity GHB binding sites with different**
410 **sensitivity to GHB radioligands by *in vitro* autoradiography in brain slices from mouse cortex**
411 **and hippocampus.** Total binding is reported as fmol/mg tissue equivalents (TE) for the
412 radioligands (**A**) [^{3}H]HOCPCA (1 nM) and (**B**) [^{3}H]NCS-382 (7 nM) and (**C**) [^{3}H]GHB (30 nM) (similar
413 specific activities). Non-specific binding was not detected in the presence of 1 mM GHB or 1 mM
414 HOCPCA for any of the radioligands (not shown). Data is presented as mean ± SD of four biological
415 replicates each performed in three technical replicates.
416
417 **Figure 6: Representative results of autoradiographic determination of K_d and B_{max} values by**
418 **homologous competitive displacement of [^{3}H]HOCPCA and [^{3}H]NCS-382 in mouse cortical**
419 **sections at pH 6.0 and pH 7.4 in order to illustrate the influence of pH on affinity of radioligands.**
420 (K_d and B_{max} were calculated using the same compound as radioligand and competitor, through
421 initial determination of K_i values[22]). (**A**) Autoradiograms with optimal signal-to-noise ratio for 1
422 nM [^{3}H]HOCPCA binding at pH 6.0. (**B**) Changing buffer pH to 7.4 requires a higher [^{3}H]HOCPCA
423 concentration (8 nM) to reach significant binding levels. (**C**) Resulting log-concentration binding
424 curves; mean ± SEM. (**D**) 5 nM [^{3}H]NCS-382 binding at pH 6.0 results in low non-specific binding,
425 whereas (**E**) 40 nM [^{3}H]NCS-382 is insufficient to obtain binding at pH 7.4. (**F**) Resulting log-
426 concentration binding curves; mean ± SEM. Data was obtained from 3-4 biological replicates each
427 performed in 3-5 technical replicates, only [^{3}H]NCS-382 experiments at pH 7.4 were performed
428 with only 2 biological replicates. For both radioligands, 1 mM GHB was used for the
429 determination of non-specific binding. For details on analysis and calculation of K_d and B_{max}, see[9].
430 This figure has been adapted and reprinted from previous publication[9] with permission from
431 Elsevier.
432
433 **DISCUSSION:**
434 The quality of an autoradiographic assay is most often determined by the sensitivity of the
435 radioligand. A major contributing factor is the selected radioisotope, which is given by the
436 availability of known ligands or by the feasibility of specific labelling techniques to yield ligands
437 with appropriate specific activity (*i.e.*, the amount of radioactivity per unit mole of a

438 radioligand)[23] and with limited amounts of chemical degradation. A large number of radioligands
439 of known ligands are labelled with tritium[9,10,24–26], which infers several advantages. Firstly, tritium
440 (^{3}H) is characterized by a long half-life (12.43 years) promoting long-term storage of individual
441 batches. Secondly, the ligand-target interaction is not distorted by the radionuclide as ^{3}H-ligands
442 are biologically indistinguishable from their parent compounds. Tritium emits low energy β$^-$-
443 particles, which travel only short distances in tissue resulting in high spatial resolution and,
444 subsequently, greater distinction between anatomical structures[4]. Nonetheless, tritium labelling
445 can only be produced to yield moderately high specific activities. This is due to the fact that
446 available ^{3}H-sources are contaminated with non-radioactive hydrogen. Generally, the higher the
447 specific activity, the less radioligand is needed to yield sensitive detection[23]. Moreover, it should
448 be considered that ^{3}H-ligands have the possibility to undergo hydrogen exchange with water
449 depending on the stability of the ^{3}H-label. To compensate for low expression or too low specific
450 activity, iodine-125 can be used as the radionuclide[13]. The maximal specific activity of iodine-125
451 is approx. 100-fold higher than that of tritium. However, several additional considerations have
452 to be made when working with iodine-125. For instance, the addition of iodine-125 normally
453 induces structural alterations in the molecule which may impact the ligand-target interactions.
454 As iodine-125 has a half-life of 60 days, correction for daily decay should be considered for
455 specific activity and quantification of ligand-target interactions[23]. ^{125}I-ligands emit γ-photons and
456 in spite of much higher sensitivity, produce lower-resolution images. This is due to the inverse
457 relationship between resolution and the maximum energy of the isotope (as discussed below).
458 Finally, compared to tritium, increased care should be taken when handling iodine-125 due to
459 the higher energy of the radionuclide.

461 Depending on the nuclide, tissue section thickness may influence resolution. The low-energy β$^-$-
462 radiation of tritium limits its tissue reach to approx. 5 μm due to self-absorption. As a
463 consequence, quantification is not influenced by tissue thickness when the section thickness
464 exceeds 5 μm[27,28]. By contrast, radioactive decay of high-energy isotopes has a greater tissue
465 penetration, resulting in lower image resolution because ligands with a greater distance to the
466 detection medium also contribute to image formation. Consequently, thinner sections promote
467 higher resolution for high-energy radionuclides[1].

469 The establishment of an autoradiographic protocol requires knowledge of optimal binding
470 conditions (*e.g.*, buffer, pH and temperature) and pharmacological parameters of the radioligand
471 in terms of affinity and kinetics. If the radioligand has not been characterized before, exploratory
472 studies are necessary[29]. Choosing an optimal radioligand concentration is guided both by the
473 affinity of the radioligand and the abundance of binding sites. Normally, a concentration
474 reflecting 5-6 times K_d is used to make sure that all binding sites are saturated[30]. Another
475 approach aims to yield the highest ratio of total-to-non-specific binding by selecting radioligand
476 concentrations below K_d[31] and saving radioligand solution at the same time. This approach is
477 particularly useful when the binding site is highly abundant in the examined tissue since high
478 radioligand concentrations would increase the chance of oversaturating autoradiograms, as the
479 case for [^{3}H]HOCPCA and the high-affinity GHB binding sites[9]. Furthermore, in order to efficiently
480 label the whole population of the targeted protein, the radioligand should ideally bind to all
481 possible target conformations. Especially in receptor autoradiography, the use of agonists may

482 only reveal a partial number of total receptors since some might be present in low-affinity agonist
483 states. In contrast, neutral antagonists most often display affinity for all receptor states[26,29].

485 Moreover, binding experiments are generally performed under equilibrium binding conditions.
486 Therefore, the time needed to reach equilibrium binding under the desired experimental
487 conditions (fixed radioligand concentration, buffer and temperature) should be determined in
488 association experiments to ensure equilibrium binding within the scope of the experiment[4,23,30].
489 After radioligand incubation, unbound radioligand is washed off by several incubations with assay
490 buffer and typically followed by rinsing in distilled H_2O. Signal-to-noise ratios can be optimized
491 by adjusting temperature and time depending on the dissociation rate of the radioligand[26,30,31].

493 Radioligands may display binding to non-biological materials, *i.e.*, non-specific binding.
494 Radioligand binding to cellular components other than the intended target is defined as
495 unspecific binding. The contribution of unspecific binding to the total amount of radioligand
496 binding is assessed in the presence of a competing unlabelled ligand that targets the same
497 binding site as the radioligand. As the non-radioactive compound (displacer) is supplied in
498 10,000-fold excess, it occupies the binding site and the radioligand can only bind to off-target
499 sites[26,31,32]. Crucially, the unlabelled compound should be of a different chemical structure than
500 the radioligand since this lowers the risk of displacing both specific as well as non-specific
501 binding[23]. Non-specific binding arising from binding to membranes can be a major problem
502 especially in the case of fairly lipophilic radioligands. In some cases, extensive washing
503 procedures may remove non-receptor bound radioligand and therefore improve the specific
504 binding ratios[29].

506 When choosing an assay buffer, it is crucial to consider the effect of ionic strength and pH on the
507 ligand-target interaction. Especially electrostatic interactions between polar ligands and
508 hydrophilic components of binding sites are influenced by the ionic strength of the buffer.
509 Therefore, supplementation with monovalent or divalent ions may impact the effective affinity
510 constant[23,33]. If the optimal buffer composition for the studied ligand-target interaction is
511 unknown, different common buffers should be explored in pilot experiments. Buffers may also
512 be supplemented with anti-oxidants such as ascorbic acid and inhibitors of degrading
513 enzymes[29,34]. Moreover, the ionization of specific groups within the binding site or on the ligand
514 itself is influenced by pH and has critical effects on the equilibrium binding constant, the kinetic
515 rate constants and non-specific binding[23,33]. For example, probing the high-affinity GHB binding
516 site with different GHB radioligands nicely illustrates the importance of pH on this binding target
517 (**Figure 6**). Characterizing the optimal pH for the ligand-receptor interaction may also give clues
518 about the importance of the target in relation to its biological relevance.

520 Another critical factor in digital autoradiography is the exposure time, *i.e.*, the time needed to
521 achieve quantifiable autoradiograms by exposing the radiolabelled tissue sections to phosphor
522 imaging plates. Estimates are based on the amount of radioactivity in the sample, the energy and
523 half-life of the isotope as well as the desired signal-to-noise ratio. In particular, prolonged
524 exposure time results in saturated images and high background signal. Elevated background
525 signal can be reduced by storing cassettes within lead-shielded environments to avoid cosmic

526 radiation[1,4]. Nevertheless, if suboptimal autoradiograms are achieved, the specimen can be
527 exposed multiple times, provided that the ligand-target complex is fixed and the half-life of the
528 radionuclide allows it.
529
530 Phosphor imaging plates can be reused and have a long lifespan when handled correctly, *i.e.*,
531 bending should be avoided and plates should be stored in a dry environment. The handling of
532 phosphor imaging plates is guided by their sensitivity to light and cosmic radiation. Thus, it is
533 important to erase the plate prior to every use in order to minimize background signal. Exposure
534 of radiolabelled tissue sections to the imaging plates is done in radiation-shielded cassettes
535 completely devoid of light. When transferring the plate to the scanner at the end of the exposure
536 time, any ambient light should also be avoided as even short contact with white light reduces
537 accumulated signal. Furthermore, plates should be scanned immediately after the removal of the
538 specimen to avoid signal fading. A drawback of using phosphor imaging plates is the potential
539 appearance of artefacts and residual 'ghost images' after repeated usage of the plates[1].
540
541 Working with tritium requires imaging plates without a protective coating to allow the low energy
542 radiation to reach the phosphor crystals. Tritium-sensitive phosphor imaging plates are therefore
543 more sensitive to contamination or damage due to incorrect handling. Once contaminated,
544 tritium-sensitive plates cannot be cleaned and need to be replaced. Fixation of the ligand-target
545 complex with PFA vapour reduces potential contamination of the plate, lengthening its lifespan.
546 Moreover, dehydration of the tissue subsequent to fixation is a crucial step since tritium sensitive
547 plates are sensitive to moisture. Due to its delicate nature, tritium-sensitive plates should not be
548 used for other isotopes[1,4]. In contrast, the plates for high-energy isotopes such as iodine-125 are
549 more robust and their surface can even be cleaned by wiping with 70% ethanol.
550
551 Traditionally, radiosensitive film has been used for the spatial recording of radioactive decay.
552 While images with high resolution can be obtained, film autoradiography has several limitations.
553 Besides the necessity of hazardous chemicals and a darkroom for development, X-ray film is
554 characterized by a narrow dynamic range. Therefore, it may be necessary to expose radiolabelled
555 sections repeatedly with different exposure times in order to achieve quantifiable non-saturated
556 images[35]. Moreover, X-ray film exhibits limited sensitivity resulting in sustained exposure times
557 for specimen labelled with low energy isotopes, *i.e.* tritium decay may require several months of
558 exposure. Low sensitivity combined with small linear range makes the technique extremely time
559 consuming, especially when optimal assay conditions have to be determined first[1,35].
560
561 With the development of phosphor imaging plates, several of these limitations have been
562 addressed[35–37]. The imaging plates serve to temporarily store images of radioactive decay,
563 representing the spatial arrangement of radioligand in the tissue specimen. Photostimulable
564 $BaFBr:Eu^{2+}$ phosphor crystals are used to capture the radioactive energy emitted by the sample,
565 as high energy radiation (*e.g.*, X-rays, gamma rays or beta particles) results in the excitation of
566 Eu^{2+} to Eu^{3+} and consequent trapping of the released electron in the phosphor lattice[4,37]. Exposing
567 the imaging plate to visible or infrared light reverses the reaction, *i.e.*, the trapped electron is
568 released and during the transformation of Eu^{3+} to Eu^{2+} luminescence is emitted. The emitted light
569 is proportional to the amount of radioactivity and its detection by a photomultiplier enables the

570   creation of a digital autoradiogram[37]. This system provides an increase in sensitivity accompanied
571   by a marked reduction in exposure time from month to days[3]. On top of that, the linear dynamic
572   range is considerably increased, which reduces the chance of oversaturated images. Linearity is
573   given within four to five orders of magnitude and has been validated repeatedly[3,35–38]. Although
574   film autoradiography still provides superior spatial resolution, efforts in scanning technology
575   resulted in the improvement of resolution from 300 to 25 µm (pixel size), allowing the detailed
576   differentiation between anatomical regions[3]. Overall, phosphor imaging plates are facilitating the
577   acquirement of digital autoradiograms both due to an increased linear range and sensitivity.
578   Reduced exposure time and a simplified development technique significantly lead to decreased
579   time for data analysis allowing higher throughput.
580
581   Compared to autoradiography, useful pharmacological parameters such as affinity and density
582   are also commonly characterized by the application of radioligands in tissue homogenate binding
583   assays. This method has the advantage of producing results by measuring β-emitted radioactive
584   decay with a liquid scintillation detector in an efficient manner[2]. Being performed in a multi-well
585   approach, *e.g.,* in 96-well microtiter plates, such assays are useful for screening of libraries of
586   compounds and for a larger number of concentration-dependent relationships. On top of that,
587   conducting saturation analysis with this setup is often more feasible compared to
588   autoradiography, which displays a risk of oversaturated images with high radioligand
589   concentrations. However, performing homologous displacement of a fixed low radioligand
590   concentration with non-radioactive ligands in order to obtain K_d and B_{max} circumvents the
591   problem of oversaturated images (**Figure 6**)[22]. Homogenate binding and autoradiography
592   produce similar estimates for ligand affinity constants whereas tissue density of the protein of
593   interest may be underestimated in homogenate binding. Thus, it has been proposed that cell
594   membrane disruption concomitant with tissue homogenisation might result in receptor loss or
595   altered binding conditions[3,33]. Moreover, errors in tissue dissection might produce homogenates
596   contaminated with tissue from adjacent brain regions. In comparison, even complex binding
597   patterns in small nuclei are visualized and differentiable due to the spatial anatomical resolution
598   in autoradiography[3,33].
599
600   Immunohistochemistry also visualizes the distribution of a protein of interest anatomically. The
601   method is capable of producing images with high anatomical resolution, as discrete tissue
602   components can be identified at cellular level and even subcellular levels using electron
603   microscopy. Expression levels are assessed based on the intensity of the staining. Nonetheless,
604   absolute quantification of expression levels is difficult due to the lack of appropriate reference
605   standards[39]. Moreover, immunohistochemistry is dependent on the availability of a selective,
606   well-validated antibody which is often a problem in receptor research.
607
608   Before deciding on performing *in vitro* autoradiography, several considerations need to be made.
609   First of all, post-mortem tissue preparation including sectioning as well as repeated freezing and
610   thawing might influence the preservation of binding sites[2]. Furthermore, the method depends
611   on the availability of an adequate radioligand, which displays high affinity and selectivity for the
612   target in question[2]. The radioligand should not display significant binding to off-target sites, and
613   it should also demonstrate a favourable kinetic profile. This is necessary because the ligand-

target complex must stay intact during the scope of the experiment. Moreover, when suitable non-radioactive compounds exist, the introduction of the radionuclide might become a critical factor. Thus, the molecule of interest should be equipped with suitable functional groups for efficient radiolabelling, which enables production of radioligands with sufficiently high specific activity and chemical stability[40]. Another disadvantage of *in vitro* autoradiography is that the method only allows the use of an animal once. More elegantly is the extension to *in vivo* imaging methods such as position emission tomography (PET), which enables repeated scanning of the same animal and determination of occupancy and dynamic binding characteristics. PET is especially valuable for the study of higher mammals[41] and for dose optimization in pre-clinical studies [42–44].

Several modifications of the autoradiographic technique extend its application both in terms of the characterization of pharmacological targets in healthy and diseased states as well as in drug discovery and development. First of all, recent advances in imaging technology have led to the development of real-time autoradiography. Gas detectors of α/β-particles obviate the need for imaging plates or film by the direct measurement of disintegrations, thereby producing fast digital autoradiograms[45].

Moreover, *in vitro* autoradiography enables studies of the functionality of G protein-coupled receptors (GPCRs) on top of information about their anatomical distribution in post-mortem tissues. This variant of the method involves incubation of tissue sections with a radioactively labelled analogue of guanosine triphosphate (GTP), *i.e.,* [^{35}S]guanosine 5'-γ-thiotriphosphate ([^{35}S]GTPγS), together with a non-radioactive agonist of the GPCR. When the agonist binds and elicits a response of the GPCR, the incorporation of [^{35}S]GTPγS can be localized and quantified via autoradiography, which reflects only the activated receptor population[2,46,47].

Ex vivo autoradiography represents another version of the technique, which assesses the regional binding of a radioligand after administration to a live experimental animal. Following the sacrifice of the animal, cryosectioning of the tissue in question, and autoradiographic exposure result in autoradiograms which reflect the radioligand binding *in vivo*[2]. *Ex vivo* autoradiography is commonly employed within drug discovery and development programs in order to gain information on the pharmacokinetic profile of a lead compound, *i.e.,* its absorption, distribution, metabolism and excretion (ADME). Particularly whole-body autoradiography provides insight about drug distribution to all organs and tissues. However, determination of non-specific binding and quantification is more difficult compared to *in vitro* autoradiography due to possible metabolism and degradation of the radioligand and no means for washing away unbound ligand[48].

Autoradiography is also used for preliminary testing and characterization of PET ligands[4]. The high-energy radionuclides carbon-11 and fluorine-18 are most often used for PET ligands. PET is a prominent, non-invasive application for radioligands because quantifiable 3D images of the radioligand binding in a living animal can be obtained[11,40,49].

In vitro autoradiography using phosphor imaging plates represents a valuable assay method for

658 the pharmacological characterization of ligand-target interactions. The method produces
659 reproducible results by the employment of a relatively fast and simple protocol once optimal
660 assay conditions have been established. Anatomical distribution of a protein of interest is
661 determined within its native microenvironment, which allows the study of its physiological,
662 pharmacological and pathological role in healthy and diseased post-mortem tissue of
663 experimental animals as well as humans[2,47].
664

669

670 **DISCLOSURES:**
671 The authors declare no conflicts of interest.
672

673 **REFERENCES:**
674 1.   Upham, L. V. & Englert, D. F. in *Handbook of Radioactivity Analysis* 1063–1127 (Elsevier
675 Inc., 2003).
676 2.   Manuel, I. *et al.* Neurotransmitter receptor localization: From autoradiography to imaging
677 mass spectrometry. *ACS Chemical Neuroscience.* **6,** 362–373 (2015).
678 3.   Pavey, G. M., Copolov, D. L. & Dean, B. High-resolution phosphor imaging: validation for
679 use with human brain tissue sections to determine the affinity and density of radioligand binding.
680 *Journal of Neuroscience Methods.* **116,** 157–163 (2002).
681 4.   Davenport, A. P. *Receptor Binding Techniques*. **897,** (Humana Press, 2012).
682 5.   Busardò, F. P., Kyriakou, C., Napoletano, S., Marinelli, E. & Zaami, S. Clinical applications
683 of sodium oxybate (GHB): from narcolepsy to alcohol withdrawal syndrome. *European Review for*
684 *Medical and Pharmacological Sciences.* **19,** 4654–4663 (2015).
685 6.   Wong, C. G. T., Gibson, K. M. & Snead, O. C. I. From the street to the brain: neurobiology
686 of the recreational drug γ-hydroxybutyric acid. *Trends in Pharmacological Sciences.* **25,** 29–34
687 (2004).
688 7.   Benavides, J. *et al.* High affinity binding site for γ-hydroxybutyric acid in rat brain. *Life*
689 *Sciences.* **30,** 953–961 (1982).
690 8.   Hechler, V., Gobaille, S. & Maitre, M. Selective distribution pattern of γ-hydroxybutyrate
691 receptors in the rat forebrain and midbrain as revealed by quantitative autoradiography. *Brain*
692 *Research.* **572,** 345–348 (1992).
693 9.   Klein, A. B. *et al.* Autoradiographic imaging and quantification of the high-affinity GHB
694 binding sites in rodent brain using 3H-HOCPCA. *Neurochemistry International* **100,** 138–145
695 (2016).
696 10.   Gould, G. G., Mehta, A. K., Frazer, A. & Ticku, M. K. Quantitative autoradiographic analysis
697 of the new radioligand [3H](2*E*)-(5-hydroxy-5,7,8,9-tetrahydro-6*H*-benzo[α][7]annulen-6-
698 ylidene) ethanoic acid ([3H]NCS-382) at γ-hydroxybutyric acid (GHB) binding sites in rat brain.
699 *Brain Research.* **979,** 51–6 (2003).
700 11.   Jensen, C. H. *et al.* Radiosynthesis and evaluation of [11C]3-hydroxycyclopent-1-

enecarboxylic acid as potential PET ligand for the high-affinity γ‑hydroxybutyric acid binding sites. *ACS Chemical Neuroscience.* 22–27 (2017).

12.   Castelli, M. P., Mocci, I., Langlois, X., Gommeren, W. & Luyten, W. H. M. L. Quantitative autoradiographic distribution of γ-hydroxybutyric acid binding sites in human and monkey brain. *Molecular Brain Research.* **78,** 91–99 (2000).

13.   Wellendorph, P. *et al.* Novel radioiodinated γ-hydroxybutyric acid analogues for radiolabeling and photolinking of high-affinity γ-hydroxybutyric acid binding sites. *Journal of Pharmacology and Experimental Therapeutics.* **335,** 458–464 (2010).

14.   Vogensen, S. B. *et al.* New synthesis and tritium labeling of a selective ligand for studying high-affinity γ-hydroxybutyrate (GHB) binding sites. *Journal of Medicinal Chemistry* **56,** 8201–8205 (2013).

15.   Mehta, A. K., Muschaweck, N. M., Maeda, D. Y., Coop, A. & Ticku, M. K. Binding characteristics of the γ-hydroxybutyric acid receptor antagonist [3H](2*E*)-(5-hydroxy-5,7,8,9-tetrahydro-6*H*-benzo[a][7]annulen-6-ylidene) ethanoic acid in the rat brain. *Journal of Pharmacology and Experimental Therapeutics.* **299,** 1148–53 (2001).

16.   Kaupmann, K. *et al.* Specific γ-hydroxybutyrate-binding sites but loss of pharmacological effects of γ-hydroxybutyrate in GABA$_{B(1)}$-deficient mice. *Neuroscience* **18,** 2722–2730 (2003).

17.   Bay, T., Eghorn, L. F., Klein, A. B. & Wellendorph, P. GHB receptor targets in the CNS: Focus on high-affinity binding sites. *Biochemical Pharmacology.* **87,** 220–228 (2014).

18.   Paxinos, G. & Franklin, K. B. J. *The mouse brain in stereotaxic coordinates*. (Academic Press, 2008).

19.   Carletti, R., Tacconi, S., Mugnaini, M. & Gerrard, P. Receptor distribution studies. *Current Opinion in Pharmacology.* **35,** 94–100 (2017).

20.   Wellendorph, P. *et al.* Novel cyclic γ-hydroxybutyrate (GHB) analogs with high affinity and stereoselectivity of binding to GHB sites in rat brain. *Journal of Pharmacology and Experimental Therapeutics.* **315,** 346–351 (2005).

21.   Coenen, H. H. *et al.* Consensus nomenclature rules for radiopharmaceutical chemistry — Setting the record straight. *Nuclear Medicine and Biologly.* **55,** v–xi (2017).

22.   DeBlasi, A., O'Reilly, K. & Motulsky, H. J. Calculating receptor number from binding experiments using same compound as radioligand and competitor. *Trends in Pharmacological Science.* **10,** 227–229 (1989).

23.   Hulme, E. C. *Receptor-ligand interactions: a practical approach*. (RL Press at Oxford University Press, 1992).

24.   Holm, P. *et al.* Plaque deposition dependent decrease in 5-HT$_{2A}$ serotonin receptor in AβPPswe/ PS1dE9 amyloid overexpressing mice. *Journal of Alzheimer's Disease.* **20,** 1201–1213 (2010).
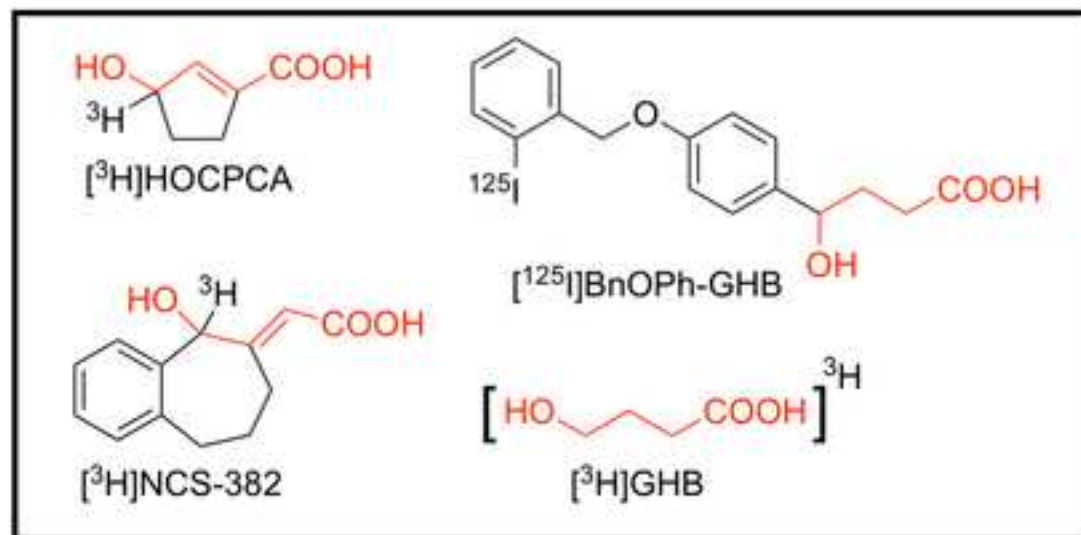
25.   Thomsen, C. & Helboe, L. Regional pattern of binding and c-Fos induction by (R)- and (S)-citalopram in rat brain. *Neurochemistry* **14,** 2411–2414 (2003).
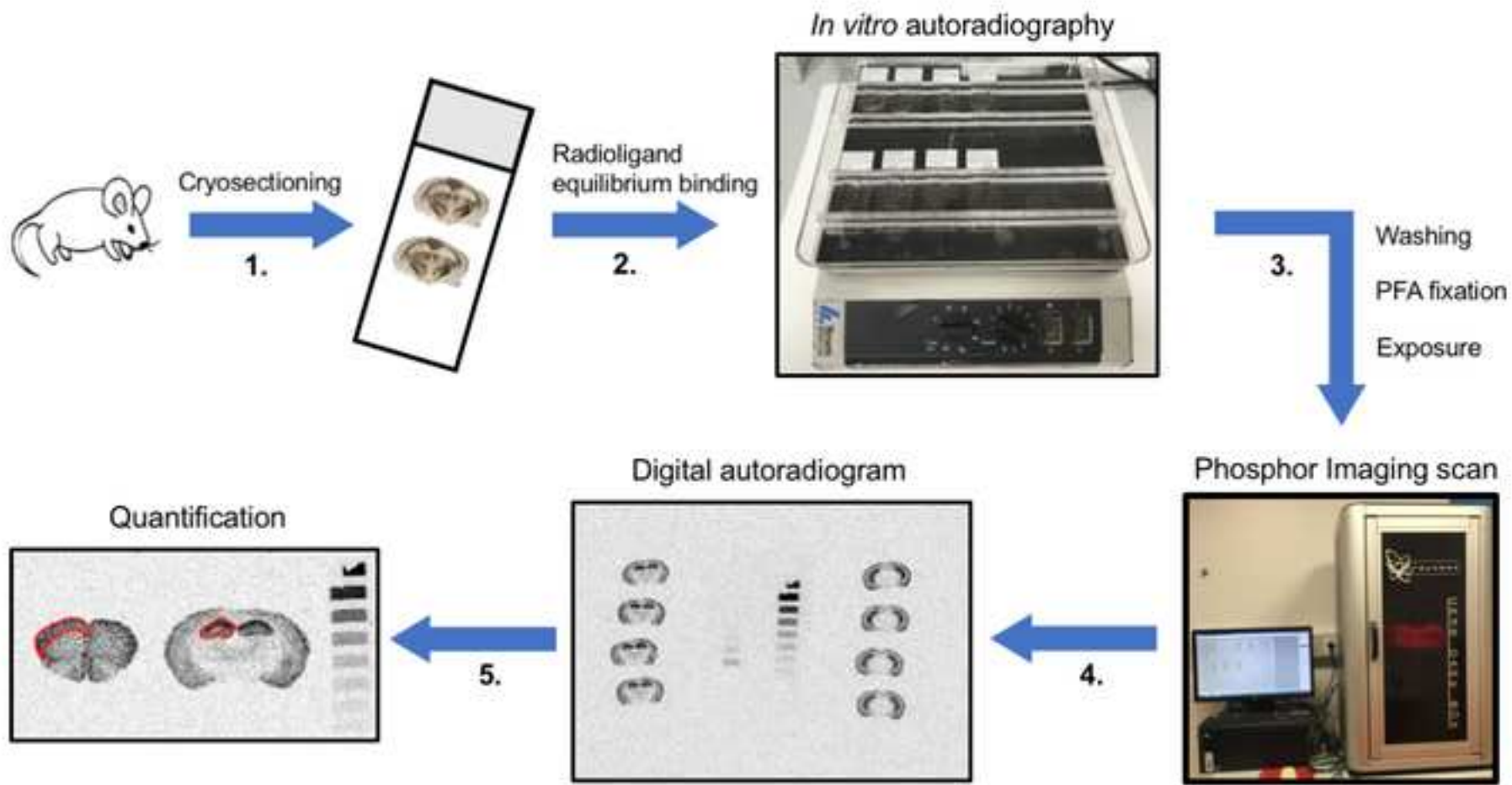
26.   López-Giménez, J. F., Mengod, G., Alacios, J. M. & Vilaró, M. T. Selective visualization of rat brain 5-HT$_{2A}$ receptors by autoradiography with [3H]MDL 100 ,907. *Naunyn-Schmiedeberg's Archieves of Pharmacology.* **356,** 446–454 (1997).
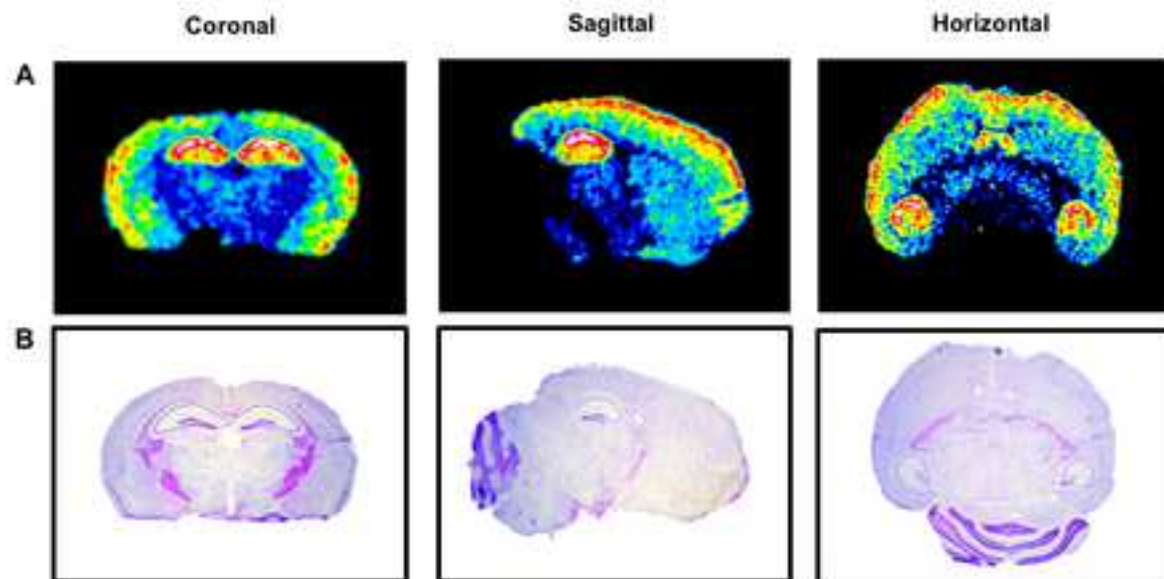
27.   Alexander, G. M., Schwartzman, R. J., Bell, R. D., Yu, J. & Renthal, A. Quantitative measurement of local cerebral metabolic rate for glucose utilizing tritiated 2-deoxyglucose. *Brain Research.* **223,** 59–67 (1981).
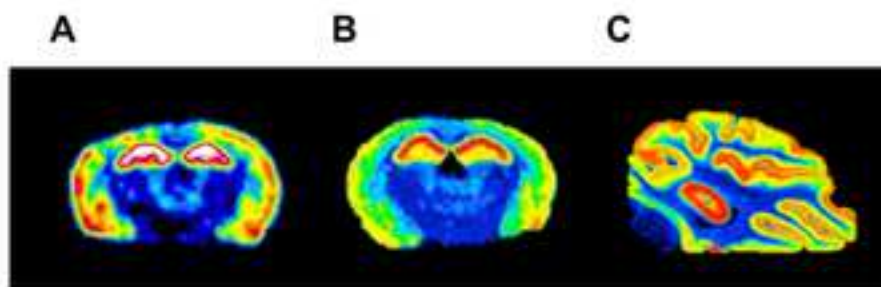
28.   Kuhar, M. J. & Unnerstall, J. R. Quantitative receptor mapping by autoradiography: some current technical problems. *Trends in Neurosciences.* 49–53 (1985).

29.   Kuhar, M. J., De Souza, E. B. & Unnerstall, J. R. Neurotransmitter receptor mapping by autoradiography and other methods. *Annual Review of Neuroscience.* 27–59 (1986).

30.   Chen, H.-T., Clark, M. & Goldman, D. Quantitative Autoradiography of ^{3}H-Paroxetine Binding Sites in Rat Brain. *Journal of Pharmacological and Toxicological Methods.* **27,** 209–216 (1992).

31.   Herkenham, M. & Pert, C. B. Light microscopic localization of brain opiate receptors: a general autoradiographic method which preserves tissue quality. *Journal of Neuroscience.* **2,** 1129–49 (1982).

32.   Heimer, L. & Záborszky, L. *Neuroanatomical Tract-Tracing Methods 2 - Recent progress.* (Plenum Press, 1989).

33.   Vessotskie, J. M., Kung, M. P., Chumpradit, S. & Kung, H. F. Quantitative autoradiographic studies of dopamine D_3 receptors in rat cerebellum using [^{125}I]S(-)5-OH-PIPAT. *Brain Research.* **778,** 89–98 (1997).

34.   Klein, A. B. *et al.* 5-HT$_{2A}$ and mGLU$_2$ receptor binding levels are related to differences in impulsive behavior in the roman low- (RLA) and high- (RHA) avoidance rat strains. *Neuroscience* **263,** 36–45 (2014).

35.   Johnston, R. F., Pickett, S. C. & Barker, D. L. Autoradiography using storage phosphor technology. *Electrophoresis* **11,** 355–360 (1990).

36.   Ito, T., Suzuki, T., Lim, D. K., Wellman, S. E. & Ho, I. K. A novel quantitative receptor autoradiography and in situ hybridization histochemistry technique using storage phosphor screen imaging. *Journal of Neuroscience Methods* **59,** 265–271 (1995).

37.   Amemiya, Y. & Miyahara, J. Imaging plate illuminates many fields. *Nature* **336,** 89–90 (1988).

38.   Kanekal, S., Sahai, A., Jones, R. E. & Brown, D. Storage-phosphor autoradiography: a rapid and highly sensitive method for spatial imaging and quantitation of radioisotopes*. *Journal of Pharmacological and Toxicological Methods.* 171–178 (1995).

39.   Taylor, C. R. & Levenson, R. M. Quantification of immunohistochemistry — issues concerning methods , utility and semiquantitative assessment II. *Histopathology* **49,** 411–424 (2011).

40.   Uhl, P., Fricker, G., Haberkorn, U. & Mier, W. Radionuclides in drug development. *Drug Discovery Today.* **20,** 198–208 (2015).

41.   Schmidt, K. C. & Smith, C. B. Resolution, sensitivity and precision with autoradiography and small animal positron emission tomography: Implications for functional brain imaging in animal research. *Nuclear Medicine and Biolology.* **32,** 719–725 (2005).

42.   Piel, M., Vernaleken, I. & Rösch, F. Positron emission tomography in CNS drug discovery and drug monitoring. *Journal of Medicinal Chemistry.* **57,** 9232–9258 (2014).

43.   Kristensen, J. L. & Herth, M. M. *In vivo* imaging in drug discovery. *Drug Design and Discovery.* (CRC Press, Taylor & Francis Grou), 119-135 (2017).

44.   Cunha, L., Szigeti, K., Mathé, D. & Metello, L. F. The role of molecular imaging in modern drug development. *Drug Discovery Today* **19,** 936–948 (2014).

45.   Bailly, C. *et al.* Comparison of Immuno-PET of CD138 and PET imaging with ^{64}CuCl$_2$ and ^{18}F-FDG in a preclinical syngeneic model of multiple myeloma. *Oncotarget* **9,** 9061–9072 (2018).
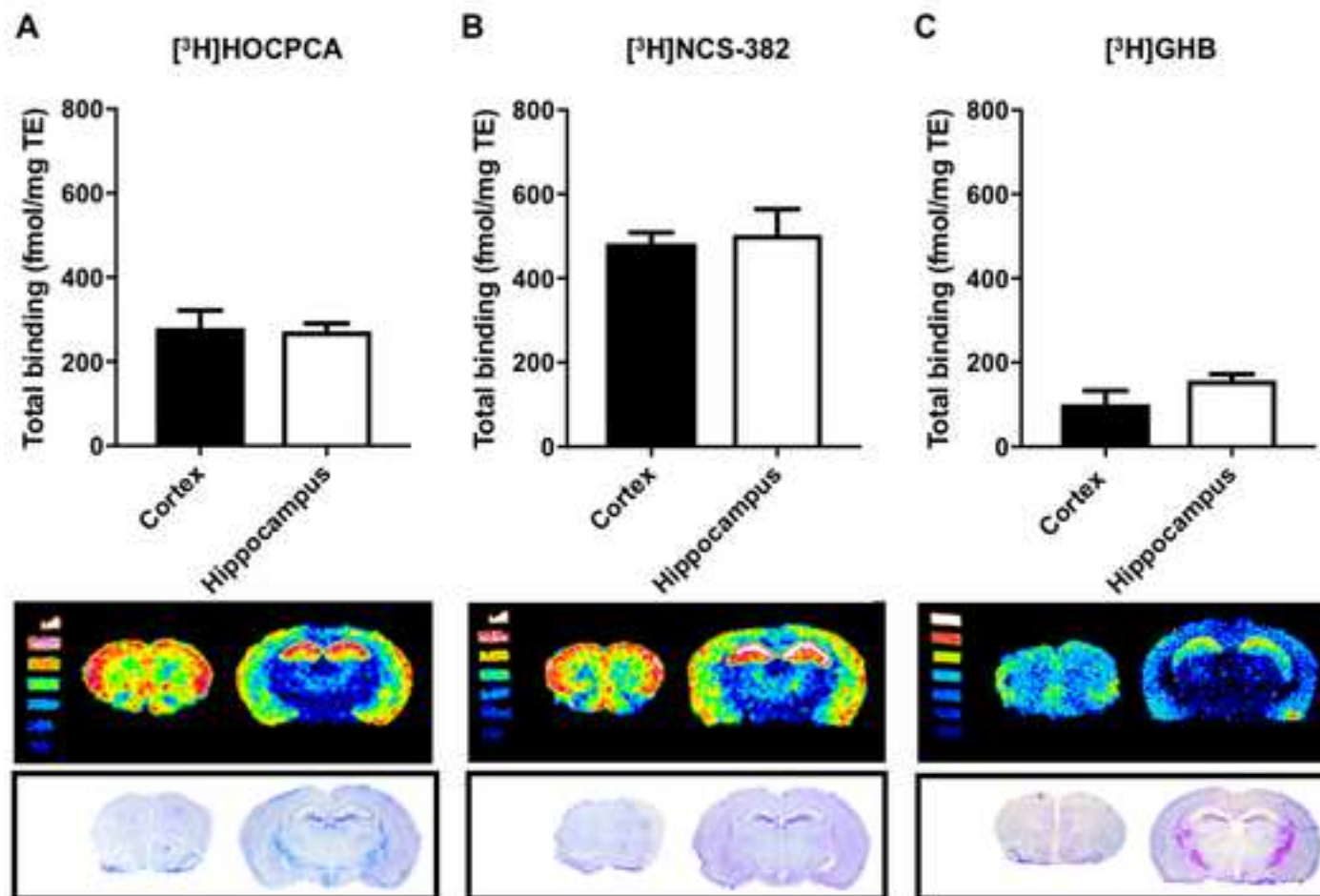
789 46.   Sóvágó, J., Makkai, B., Gulyás, B. & Hall, H. Autoradiographic mapping of dopamine-D_2/D_3
790 receptor stimulated [^{35}S]GTPγS binding in the human brain. *European Journal of Neuroscience.*
791 **22,** 65–71 (2005).
792 47.   Sóvágó, J., Dupuis, D. S., Gulyás, B. & Hall, H. An overview on functional receptor
793 autoradiography using [^{35}S]GTPγS. *Brain Research Reviews.* **38,** 149–164 (2001).
794 48.   Solon, E. G. Use of radioactive compounds and autoradiography to determine drug tissue
795 distribution. *Chemical Research in Toxicology.* **25,** 543–555 (2012).
796 49.   Donnelly, D. J. Small molecule PET tracers in drug discovery. *Seminars in Nuclear Medicine*
797 **47,** 454–460 (2017).
798

Figure 1

Figure 1

In vitro autoradiography

Cryosectioning

Radioligand equilibrium binding

1.

2.

3.

Washing

PFA fixation

Exposure

Phosphor Imaging scan

Digital autoradiogram

Quantification

5.

4.

Figure 3

Figure 4 revised

Figure 5

Click here to access/download;Figure;Figure 5.tiff ±

A [³H]HOCPCA

B [³H]NCS-382

C [³H]GHB

Figure 6

Click here to access/download;Figure;Figure 6.tiff ⬇

A [³H]HOCPCA; pH 6.0

B [³H]HOCPCA; pH 7.4

C [³H]HOCPCA inhibition curves

D [³H]NCS-382; pH 6.0

E [³H]NCS-382; pH 7.4

F [³H]NCS-382 inhibition curves

Name of Material/ Equipment	Company	Catalog Number	Comments/Description
Absolute ethanol	Merck Millipore	107017	
Acetic acid	Sigma-Aldrich	A6283	
BAS-TR2040 Imaging Plate	GE Healthcare Life Science	28956481	20x40 cm - Sensitive to tritium
Cresyl violet acetate	Sigma-Aldrich	C5042-10G	
DPX (non-aqueous mounting medium for microscop	Merck Millipore	100579	
O.C.T. Compound, 12 x 125 mL	Sakura	4583	Tissue-Tek
Paraformaldehyde	Sigma-Aldrich	16005-1KG-R	
Superfrost Plus slides	VWR	631-9483	microscope slides
Tissue-Tek Manual Slide Staining Set	Sakura Finetek Denmark ApS	4451	
Tritium Standard on Glas	American Radiolabeld Chemicals, Inc.	ART 0123	
Xylene substitute	Sigma-Aldrich	A5597	

jove
JOURNAL OF
VISUALIZED EXPERIMENTS

1 Alewife Center #200
Cambridge, MA 02140
tel. 617.945.9051
www.jove.com

ARTICLE AND VIDEO LICENSE AGREEMENT

Title of Article: Autoradiography as a simple and powerful method for visualization and characterization of pharmacological targets

Author(s): Nane Griem-Krey, Anders B. Klein, Matthias M. Herth, Petrine Wellendorph

Item 1: The Author elects to have the Materials be made available (as described at http://www.jove.com/publish) via:

[x] Standard Access   [ ] Open Access

Item 2: Please select one of the following items:

[x] The Author is **NOT** a United States government employee.

[ ] The Author is a United States government employee and the Materials were prepared in the course of his or her duties as a United States government employee.

[ ] The Author is a United States government employee but the Materials were NOT prepared in the course of his or her duties as a United States government employee.

ARTICLE AND VIDEO LICENSE AGREEMENT

1.   **Defined Terms.** As used in this Article and Video License Agreement, the following terms shall have the following meanings: "**Agreement**" means this Article and Video License Agreement; "**Article**" means the article specified on the last page of this Agreement, including any associated materials such as texts, figures, tables, artwork, abstracts, or summaries contained therein; "**Author**" means the author who is a signatory to this Agreement; "**Collective Work**" means a work, such as a periodical issue, anthology or encyclopedia, in which the Materials in their entirety in unmodified form, along with a number of other contributions, constituting separate and independent works in themselves, are assembled into a collective whole; "**CRC License**" means the Creative Commons Attribution-Non Commercial-No Derivs 3.0 Unported Agreement, the terms and conditions of which can be found at: http://creativecommons.org/licenses/by-nc-nd/3.0/legalcode; "**Derivative Work**" means a work based upon the Materials or upon the Materials and other pre-existing works, such as a translation, musical arrangement, dramatization, fictionalization, motion picture version, sound recording, art reproduction, abridgment, condensation, or any other form in which the Materials may be recast, transformed, or adapted; "**Institution**" means the institution, listed on the last page of this Agreement, by which the Author was employed at the time of the creation of the Materials; "**JoVE**" means MyJove Corporation, a Massachusetts corporation and the publisher of The Journal of Visualized Experiments; "**Materials**" means the Article and / or the Video; "**Parties**" means the Author and JoVE; "**Video**" means any video(s) made by the Author, alone or in conjunction with any other parties, or by JoVE or its affiliates or agents, individually or in collaboration with the Author or any other parties, incorporating all or any portion of the Article, and in which the Author may or may not appear.

2.   **Background.** The Author, who is the author of the Article, in order to ensure the dissemination and protection of the Article, desires to have the JoVE publish the Article and create and transmit videos based on the Article. In furtherance of such goals, the Parties desire to memorialize in this Agreement the respective rights of each Party in and to the Article and the Video.

3.   **Grant of Rights in Article.** In consideration of JoVE agreeing to publish the Article, the Author hereby grants to JoVE, subject to **Sections 4** and **7** below, the exclusive, royalty-free, perpetual (for the full term of copyright in the Article, including any extensions thereto) license (a) to publish, reproduce, distribute, display and store the Article in all forms, formats and media whether now known or hereafter developed (including without limitation in print, digital and electronic form) throughout the world, (b) to translate the Article into other languages, create adaptations, summaries or extracts of the Article or other Derivative Works (including, without limitation, the Video) or Collective Works based on all or any portion of the Article and exercise all of the rights set forth in (a) above in such translations, adaptations, summaries, extracts, Derivative Works or Collective Works and (c) to license others to do any or all of the above. The foregoing rights may be exercised in all media and formats, whether now known or hereafter devised, and include the right to make such modifications as are technically necessary to exercise the rights in other media and formats. If the "Open Access" box has been checked in **Item 1** above, JoVE and the Author hereby grant to the public all such rights in the Article as provided in, but subject to all limitations and requirements set forth in, the CRC License.

ARTICLE AND VIDEO LICENSE AGREEMENT

joVE
JOURNAL OF
VISUALIZED EXPERIMENTS

1 Alewife Center #200
Cambridge, MA 02140
tel. 617.945.9051
www.jove.com

4.   **Retention of Rights in Article.** Notwithstanding the exclusive license granted to JoVE in **Section 3** above, the Author shall, with respect to the Article, retain the non-exclusive right to use all or part of the Article for the non-commercial purpose of giving lectures, presentations or teaching classes, and to post a copy of the Article on the Institution's website or the Author's personal website, in each case provided that a link to the Article on the JoVE website is provided and notice of JoVE's copyright in the Article is included. All non-copyright intellectual property rights in and to the Article, such as patent rights, shall remain with the Author.

5.   **Grant of Rights in Video – Standard Access.** This **Section 5** applies if the "Standard Access" box has been checked in **Item 1** above or if no box has been checked in **Item 1** above. In consideration of JoVE agreeing to produce, display or otherwise assist with the Video, the Author hereby acknowledges and agrees that, Subject to **Section 7** below, JoVE is and shall be the sole and exclusive owner of all rights of any nature, including, without limitation, all copyrights, in and to the Video. To the extent that, by law, the Author is deemed, now or at any time in the future, to have any rights of any nature in or to the Video, the Author hereby disclaims all such rights and transfers all such rights to JoVE.

6.   **Grant of Rights in Video – Open Access.** This **Section 6** applies only if the "Open Access" box has been checked in **Item 1** above. In consideration of JoVE agreeing to produce, display or otherwise assist with the Video, the Author hereby grants to JoVE, subject to **Section 7** below, the exclusive, royalty-free, perpetual (for the full term of copyright in the Article, including any extensions thereto) license (a) to publish, reproduce, distribute, display and store the Video in all forms, formats and media whether now known or hereafter developed (including without limitation in print, digital and electronic form) throughout the world, (b) to translate the Video into other languages, create adaptations, summaries or extracts of the Video or other Derivative Works or Collective Works based on all or any portion of the Video and exercise all of the rights set forth in (a) above in such translations, adaptations, summaries, extracts, Derivative Works or Collective Works and (c) to license others to do any or all of the above. The foregoing rights may be exercised in all media and formats, whether now known or hereafter devised, and include the right to make such modifications as are technically necessary to exercise the rights in other media and formats. For any Video to which this **Section 6** is applicable, JoVE and the Author hereby grant to the public all such rights in the Video as provided in, but subject to all limitations and requirements set forth in, the CRC License.

7.   **Government Employees.** If the Author is a United States government employee and the Article was prepared in the course of his or her duties as a United States government employee, as indicated in **Item 2** above, and any of the licenses or grants granted by the Author hereunder exceed the scope of the 17 U.S.C. 403, then the rights granted hereunder shall be limited to the maximum

rights permitted under such statute. In such case, all provisions contained herein that are not in conflict with such statute shall remain in full force and effect, and all provisions contained herein that do so conflict shall be deemed to be amended so as to provide to JoVE the maximum rights permissible within such statute.

8.   **Protection of the Work.** The Author(s) authorize JoVE to take steps in the Author(s) name and on their behalf if JoVE believes some third party could be infringing or might infringe the copyright of either the Author's Article and/or Video.

9.   **Likeness, Privacy, Personality.** The Author hereby grants JoVE the right to use the Author's name, voice, likeness, picture, photograph, image, biography and performance in any way, commercial or otherwise, in connection with the Materials and the sale, promotion and distribution thereof. The Author hereby waives any and all rights he or she may have, relating to his or her appearance in the Video or otherwise relating to the Materials, under all applicable privacy, likeness, personality or similar laws.

10.   **Author Warranties.** The Author represents and warrants that the Article is original, that it has not been published, that the copyright interest is owned by the Author (or, if more than one author is listed at the beginning of this Agreement, by such authors collectively) and has not been assigned, licensed, or otherwise transferred to any other party. The Author represents and warrants that the author(s) listed at the top of this Agreement are the only authors of the Materials. If more than one author is listed at the top of this Agreement and if any such author has not entered into a separate Article and Video License Agreement with JoVE relating to the Materials, the Author represents and warrants that the Author has been authorized by each of the other such authors to execute this Agreement on his or her behalf and to bind him or her with respect to the terms of this Agreement as if each of them had been a party hereto as an Author. The Author warrants that the use, reproduction, distribution, public or private performance or display, and/or modification of all or any portion of the Materials does not and will not violate, infringe and/or misappropriate the patent, trademark, intellectual property or other rights of any third party. The Author represents and warrants that it has and will continue to comply with all government, institutional and other regulations, including, without limitation all institutional, laboratory, hospital, ethical, human and animal treatment, privacy, and all other rules, regulations, laws, procedures or guidelines, applicable to the Materials, and that all research involving human and animal subjects has been approved by the Author's relevant institutional review board.

11.   **JoVE Discretion.** If the Author requests the assistance of JoVE in producing the Video in the Author's facility, the Author shall ensure that the presence of JoVE employees, agents or independent contractors is in accordance with the relevant regulations of the Author's institution. If more than one author is listed at the beginning of this Agreement, JoVE may, in its sole

![jove logo] 1 Alewife Center #200
Cambridge, MA 02140
tel. 617.945.9051
www.jove.com

ARTICLE AND VIDEO LICENSE AGREEMENT

discretion, elect not take any action with respect to the Article until such time as it has received complete, executed Article and Video License Agreements from each such author. JoVE reserves the right, in its absolute and sole discretion and without giving any reason therefore, to accept or decline any work submitted to JoVE. JoVE and its employees, agents and independent contractors shall have full, unfettered access to the facilities of the Author or of the Author's institution as necessary to make the Video, whether actually published or not. JoVE has sole discretion as to the method of making and publishing the Materials, including, without limitation, to all decisions regarding editing, lighting, filming, timing of publication, if any, length, quality, content and the like.

12. **Indemnification.** The Author agrees to indemnify JoVE and/or its successors and assigns from and against any and all claims, costs, and expenses, including attorney's fees, arising out of any breach of any warranty or other representations contained herein. The Author further agrees to indemnify and hold harmless JoVE from and against any and all claims, costs, and expenses, including attorney's fees, resulting from the breach by the Author of any representation or warranty contained herein or from allegations or instances of violation of intellectual property rights, damage to the Author's or the Author's institution's facilities, fraud, libel, defamation, research, equipment, experiments, property damage, personal injury, violations of institutional, laboratory, hospital, ethical, human and animal treatment, privacy or other rules, regulations, laws, procedures or guidelines, liabilities and other losses or damages related in any way to the submission of work to JoVE, making of videos by JoVE, or publication in JoVE or elsewhere by JoVE. The Author shall be responsible for, and shall hold JoVE harmless from, damages caused by lack of sterilization, lack of cleanliness or by contamination due to

the making of a video by JoVE its employees, agents or independent contractors. All sterilization, cleanliness or decontamination procedures shall be solely the responsibility of the Author and shall be undertaken at the Author's expense. All indemnifications provided herein shall include JoVE's attorney's fees and costs related to said losses or damages. Such indemnification and holding harmless shall include such losses or damages incurred by, or in connection with, acts or omissions of JoVE, its employees, agents or independent contractors.
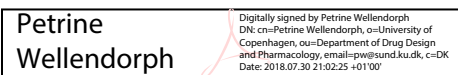
13. **Fees.** To cover the cost incurred for publication, JoVE must receive payment before production and publication the Materials. Payment is due in 21 days of invoice. Should the Materials not be published due to an editorial or production decision, these funds will be returned to the Author. Withdrawal by the Author of any submitted Materials after final peer review approval will result in a US$1,200 fee to cover pre-production expenses incurred by JoVE. If payment is not received by the completion of filming, production and publication of the Materials will be suspended until payment is received.

14. **Transfer, Governing Law.** This Agreement may be assigned by JoVE and shall inure to the benefits of any of JoVE's successors and assignees. This Agreement shall be governed and construed by the internal laws of the Commonwealth of Massachusetts without giving effect to any conflict of law provision thereunder. This Agreement may be executed in counterparts, each of which shall be deemed an original, but all of which together shall be deemed to me one and the same agreement. A signed copy of this Agreement delivered by facsimile, e-mail or other means of electronic transmission shall be deemed to have the same legal effect as delivery of an original signed copy of this Agreement.

A signed copy of this document must be sent with all new submissions. Only one Agreement is required per submission.

CORRESPONDING AUTHOR

Name: Petrine Wellendorph

Department: Drug Design and Pharmacology

Institution: University of Copenhagen

Title: Dr.

Signature: Petrine Wellendorph
Digitally signed by Petrine Wellendorph
DN: cn=Petrine Wellendorph, o=University of Copenhagen, ou=Department of Drug Design and Pharmacology, email=pw@sund.ku.dk, c=DK
Date: 2018.07.30 21:02:25 +01'00'

Date: 30/7-2018

Please submit a **signed** and **dated** copy of this license by one of the following three methods:

1. Upload an electronic version on the JoVE submission site
2. Fax the document to +1.866.381.2236
3. Mail the document to JoVE / Attn: JoVE Editorial / 1 Alewife Center #200 / Cambridge, MA 02140

612542.6   For questions, please contact us at submissions@jove.com or +1.617.945.9051.

Editorial comments:

Changes to be made by the Author(s) regarding the manuscript:

1. Please take this opportunity to thoroughly proofread the manuscript to ensure that there are no spelling or grammar issues.

We have carefully proofread the manuscript.

2. Please obtain explicit copyright permission to reuse any figures from a previous publication. Explicit permission can be expressed in the form of a letter from the editor or a link to the editorial policy that allows re-prints. Please upload this information as a .doc or .docx file to your Editorial Manager account. The Figure must be cited appropriately in the Figure Legend, i.e. "This figure has been modified from [citation]."

We have obtained the copyright permission to reuse data, specifically relating to Fig. 6. We have updated the text in the figure legend to reflect this.

3. Please provide an email address for each author.

Nane.krey@sund.ku.dk
abk@sund.ku.dk
Matthias.herth@sund.ku.dk
pw@sund.ku.dk

4. Please rephrase the Introduction to include a clear statement of the overall goal of this method.

The introduction starts with giving an overview of the purpose and the possible applications of the method. As requested, we have now further added a statement at the end in order to summarize the intentions of the paper and the overall goal of the method:

"The overall goal of this paper is to provide technical, methodological and scientific details on the autoradiography technique for informing about tissue distribution and pharmacological analysis of protein targets."

5. Please use SI abbreviations for all units: L, mL, µL, h, min, s, etc. adjusted

6. Please include a space between all numerical values and their corresponding units: 15 mL, 37 °C, 60 s; etc. adjusted

7. Please revise the protocol to contain only action items that direct the reader to do something (e.g., "Do this," "Ensure that," etc.). The actions should be described in the imperative tense in complete sentences wherever possible. Avoid usage of phrases such as "could be," "should be," and "would be" throughout the Protocol. Any text that cannot be written in the imperative tense may be added as a "Note." Please include all safety procedures and use of hoods, etc. However, notes should be used sparingly and actions should be described in the imperative tense wherever possible. Revised

8. Please add more details to your protocol steps. There should be enough detail in each step to supplement the actions seen in the video so that viewers can easily replicate the protocol. Please

ensure you answer the "how" question, i.e., how is the step performed? Alternatively, add references to published material specifying how to perform the protocol action. See examples below:

1.1: What animal and tissue are used? Please specify the euthanasia method. What is used to dissect tissue?

1.1. Euthanize mouse by cervical dislocation and immediately dissect out the brain using scissors and forceps. Directly proceed to the next step to avoid tissue damage.
1.2. Snap-freeze tissue by submersion in powdered dry ice, gaseous CO2 or isopentane. Directly transfer frozen tissue to a cryostat with the temperature set to -20 °C, or store tissue at -80 °C until processing.

1.3: Please specify the temperature.

More details about temperature have been added.

1.4 Cover tissue holder with embedding medium outside the cryostat and quickly place frozen tissue specimen in the desired orientation while the embedding medium is still liquid. For instance, mouse brain is placed vertically onto cerebellum in order to achieve rostral coronal sections. Transfer tissue holder back to the cryostat and expose embedding medium to temperatures below -10 °C for hardening.

2.3: Please break up into sub-steps.

2.3. Pre-incubate sections mounted on slides in assay buffer adjusted to target in question (for GHB protocol 50 mM KHPO4 buffer, pH 6.0 is used) by carefully applying an appropriate volume onto the slide (700 µL for 3-4 rodent coronal sections).
Note: Make sure that every section is covered completely with liquid.
2.3.1. Cover plastic trays with lid in order to avoid evaporation and pre-incubate at relevant temperature (for GHB protocol pre-incubate for 30 min at RT under constant gentle (20 rpm) shaking on a plate shaker).
2.3.2. For the determination of non-specific binding, supplement assay buffer with relevant concentration of unlabelled compound (for GHB protocol, 1 mM GHB).
Note: Pre-incubation may not be necessary.

3.6: Please describe how to stain tissue sections with cresyl violet.

4. Optional: Cresyl violet staining of tissue sections
4.1. Prepare 1% cresyl violet solution by mixing 5 g cresyl violet acetate in 500 mL deionized water (dH$_2$O) until dissolved (approximately 2 h). Filter through a filter paper using a funnel into a new 500 mL bottle. Adjust pH to 3.5–3.8.
4.2. Position slide staining set under fume hood. Prepare trays with the following solutions in white polypropylene trays (except for xylene):

      a.   50% ethanol:50% dH$_2$O
      b.   70% ethanol: 30% dH$_2$O
      c.   100% ethanol
      d.   100% ethanol
      e.   100% dH$_2$O
      f.   1% cresyl violet
      g.   0.07% acetic acid (add 175 µL acetic acid to 250 mL dH$_2$O).
      h.   100% xylene in green solvent-resistant trays

10. After you have made all the recommended changes to your protocol (listed above), please highlight 2.75 pages or less of the Protocol (including headings and spacing) that identifies the essential steps of the protocol for the video, i.e., the steps that should be visualized to tell the most cohesive story of the Protocol.

11. Please highlight complete sentences (not parts of sentences). Please ensure that the highlighted part of the step includes at least one action that is written in imperative tense. Please do not highlight any steps describing anesthetization and euthanasia.

12. Please include all relevant details that are required to perform the step in the highlighting. For

example: If step 2.5 is highlighted for filming and the details of how to perform the step are given in steps 2.5.1 and 2.5.2, then the sub-steps where the details are provided must be highlighted.

We highlighted the important steps of the protocol (yellow in the revised manuscript).

13. Please revise the table of the essential supplies, reagents, and equipment. The table should include the name, company, and catalog number of all relevant materials in separate columns in an xls/xlsx file. Please remove trademark (™) and registered (®) symbols from the Table of Equipment and Materials.

We removed trademark names, added all catalogue numbers and material.

14. References: Please do not abbreviate journal titles. adjusted

Reviewers' comments:

Reviewer #1:

Manuscript Summary:
Very nice overview of the methodology, with solid examples using multiple radioligands

Major Concerns:
The most significant concern I have is a 6 page discussion. Does seem a bit long and would be appreciated by the reader(s) if it could be streamlined I suspect

We agree that the discussion may seem lengthy. However, we do think that all considerations are relevant to get the full understanding of the technique and potential caveats. We have carefully read through the text and think that deleting a part may cut out relevant information. We also considered if additional headlines could streamline more but it is not common practice of the journal. We hope this is acceptable.

Minor Concerns: Several minor comments, with highlight to the line of the article:
Line 32-what do the authors imply with regard to an "adequate" concentration

How to choose the adequate radioligand concentration is addressed in the discussion. This would be too extensive to mention within the abstract, hence we rephrased this sentence:

"Therefore, frozen tissue sections are incubated with radioligand solution, and the binding to the target is subsequently localized by the detection of radioactive decay for example by using photosensitive film or phosphor imaging plates."

Line 56-radioisotope

"Autoradiography is easily implemented in a standard *radioisotope* laboratory given the availability of a suitable radioligand with the required pharmacological specificity…"

Line 93-determination of non-specific binding Spelling corrected

For the CAUTION segment, perhaps change legislation to regulations.

We changed it to 'regulations'.

Segment 2.1-a pencil seems risky, not a non-erasable pen or marker?

Because the slides are dipped in ethanol baths during cresyl violet staining, the writing of a marker would disappear. This has now been clarified in the protocol:

"2.1. Thaw sections for at least 30 min at room temperature (RT). Label slides with experimental conditions. Use a pencil because slides will be bathed in ethanol during subsequent staining."

Segment 2.9-eliminate moisture Spelling corrected

Segment 3.1-are currently no longer commercially available Adjusted

Segment 3.2-it is a bit confusing and there may be a better way to word this.

We have rephrased this segment from the original:

Erase tritium sensitive phosphor imaging plate immediately before usage following instructions on the phosphor imager by exposing to visible/infrared light.

To the new version:

"Erase tritium-sensitive phosphor imaging plate immediately before usage in order to remove accumulated signals from storage and to eliminate background signals. Therefore, load plate into phosphor imaging machine and expose it to visible/infrared light according to the instructions of the manufacturer"

Line 274-is performed to permanently establish the ligand-protein interaction

We have exchanged 'fixate' with 'permanently establish'

Segment 4.5, line 298 and line 310: In the first instance, it is described as technical replicates, then four biological replicates. Perhaps clarify and be consistent.

We clarified what is meant by technical and biological replicates within in the protocol.

5.6. Average the ODs of technical replicates, *i.e.* section replicates using tissue from the same animal. 5.10. Average the binding of every biological replicate by using the average of the technical replicates of each animal (obtained in step 5.6).

For any of the tritiated substrates, is there risk of exchange with non-tritiated hydrogen?

This generally depends on the compound and the stability of the ^{3}H-labelling. We added a comment in the discussion in order to point out the possibility:

"Moreover, it should be considered that ^{3}H-ligands have the possibility to undergo hydrogen exchange with water depending on the stability of the ^{3}H-label."

Line 365-what might be the case for inverse agonists? Perhaps almost as good as antagonists (affinity, no efficacy).

Inverse agonists would also be suitable as radioligands but as they preferably bind to and stabilize the inactive conformation they are not equal to neutral antagonists. Thus, we have not changed the text markedly. The only addition is the word 'neutral' to avoid confusion:

"In contrast, neutral antagonists most often display affinity for all receptor states[27,30]."

Line 470-consider changing setup to approach –

We have changed the wording to 'approach.'

Line 542-consider changing depicts to represents

This has likewise been changed.

Line 544-"a relatively fast and simple protocol". Just an editorial comment on that, it is fast and straightforward once you have done all the troubleshooting and optimization of course.

We agree with the reviewer and have adjusted the sentence accordingly:

"The method produces reproducible results by the employment of a relatively fast and simple protocol *once optimal assay conditions have been established*."

Reviewer #2:

Manuscript Summary:
This manuscript provides a thorough account of the use of autoradiography and I expect it will be of interest to the community.

Major Concerns:
None

Minor Concerns:

In the Tissue Preparation section, I would suggest adding a note to limit repeated freeze/thawing of tissue. Also, including dessicant material inside the slide boxes helps to minimize moisture that can build up on the tissues.

Added to 1.1: Note: Avoid repeated thawing/freezing to reduce tissue damage.

Added to 1.5: Note: Addition of desiccant material to slide boxes minimizes moisture build up on tissue sections.

Line 100: Consider using an isopentane instead of powdered dry ice. Cleaner?

We have added isopentane as another option for tissue freezing:

"Snap-freeze tissue by submersion in powdered dry ice, gaseous CO_2 or isopentane."

Line 140: Consider aspirating slides

Aspirating the liquid with a pipette infers a bigger risk of damaging tissue sections. We thus prefer pouring off the liquid. No changes have been made.

Line 151: Can air dry in 5 min with blower set on cold Added

"Position slides vertically in racks for air-drying for at least one hr at RT *or dry slides for 5 min with blower set to cold temperature.*"

Line 159: I think it should say "moisture" not moist. Corrected

Line 166-169: Consider using carbon-14 standards as an alternative

We just discovered that the tritium standards are commercially available again, so there is no need for alternatives. The product number etc has been added to the material list.

Line 186: densitometric is misspelled Corrected

Line 189: Figure 2, Label panels with letters or numbers

We thank for the good suggestion. We have added numbers to the figure and updated the figure legend accordingly.

Line 222: Figure 4, Use anatomically similar images for mouse, rat, pig

We totally agree with the reviewer that the different anatomical levels may be misleading. We have therefore updated the figure to include similar images for mouse, rat and pig.
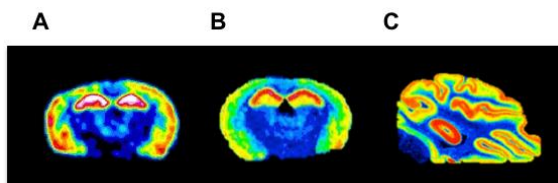
Line 230: The [3H] standards look different from each other

Regarding figure 5 – the scales look a bit different because the data was obtained in different experiments and sections were exposed to different plates, each time together with one scale.

Line 243: are expressed "at" Corrected

Line 429: should be moisture Corrected

Line 538: should be "radionuclides" and "fluorine-18" Corrected

1. Please take this opportunity to thoroughly proofread the manuscript to ensure that there are no spelling or grammar issues.

To the best of our abilities, we have proofread carefully.

2. The highlighted protocol steps are over the 2.75 page limit (including headings and spacing). Please reduce the amount of highlighted protocol steps.

We revised the highlighting of the protocol to meet the requirement.

3. For steps that are done using software, a step-wise description of software usage must be included in the step. Please mention what button is clicked on in the software, or which menu items need to be selected to perform the step.

We included more details on the specific clicks and menu items of the imaging software:

5.1.   Measure optical densities (ODs) of each calibration standard from the [3H]microscale with an image analysis software.

5.1.1.   Select an area of equal size for each point of the [3H]microscale using a tool for 'region creation' from the menu item 'region determination'. Assign a number to each selected area by clicking on 'number' under the menu item 'label'.

5.1.2.   Export OD values for each point of the calibration standard by clicking on the menu items 'file', 'export' and '2D region report'. Transfer OD values to a spreadsheet and normalize by the size of the selected area. Perform linear regression to obtain a standard curve for further densitometric analysis.

Note: Make sure that the selected areas are labelled in order to identify matching OD values and samples.

5.2.   Perform quantification of autoradiograms using the proprietary imaging software by selecting the region of interest (ROI) using a 'region creation' tool in every section and measuring its ODs. Select the same region in every section by creating a template for the region of interest, which is copied and manually adjusted to minor variations in brain anatomy for each autoradiogram. Identify the anatomy of the ROI by comparison of autoradiograms with a brain atlas (e.g.18). When multiple treatments are compared, perform the analysis blinded and randomized in order to avoid biased selection of ROIs.

5.3.   Export OD values and sizes of selected areas into a spreadsheet by clicking on the menu items 'file', 'export' and '2D region report'.

4. Calculation steps cannot be filmed unless a graphical user interface is involved and detailed software usage is provided.

We removed the highlighting from the steps involving calculations.

5. Please remove all headers from Discussion. Headers removed

6. Step 2.3: What's the temperature and time for incubation?

Preincubation temperature and time depends on the nature of the radioligand and the target. For the GHB analogue HOCPCA, pre-incubation is performed for 30 min at room temperature:

2.3.1.   Cover plastic trays with lid in order to avoid evaporation and pre-incubate at relevant temperature (for GHB protocol pre-incubate for 30 min at RT) under constant gentle (20 rpm) shaking on a plate shaker.

7. 2.5: What's the temperature and time for incubation?

Again, incubation temperature and time depends on the nature of the radioligand and the target. For the GHB analogue HOCPCA, incubation is performed for 1 h at room temperature:

2.5.   To avoid dehydration, immediately incubate sections with relevant concentration of radioligand in assay buffer under desired conditions (for GHB protocol, 1 nM [3H]HOCPCA for 1 h at RT) by covering sections completely with the radioligand solution (700 µL for 3-4 rodent coronal sections).

8. 2.8: Please write this step in imperative tense.

2.8.   Transfer slides to a fixator containing paraformaldehyde (PFA) powder for overnight fixation with PFA vapours at RT in order to protect the integrity of the ligand-target complex.